  Bull. Chem. Soc. Jpn., 58, 2786—2792 (1985) [Vol. 58, No. 10

Structure of Ni(II)- and Zn(II)-Glycinato Complexes in Aqueous Solution Determined by EXAFS Spectroscopy

Kazuhiko Ozutsumi, Toshio Yamaguchi, Hitoshi Ohtaki,* Kazuyuki Tohji,† and Yasuo Udagawa†
Department of Electronic Chemistry, Tokyo Institute of Technology at Nagatsuta, Nagatsuta-cho 4259, Midori-ku, Yokohama 227
†*Institute for Molecular Science, Myodaiji, Okazaki 444*
(Received May 18, 1985)

The EXAFS spectroscopy has been used to determine the structure of the bis(glycinato) complexes of nickel(II) and zinc(II) ions of low solubility (0.1—0.3 mol dm^{-3}) in aqueous solution. The structural parameters were evaluated by the least-squares analysis both in the reciprocal and in the real spaces on the basis of various standard samples of known structures. Analysis of the EXAFS spectra of aqueous solutions containing the bis(glycinato) complexes of nickel(II) and zinc(II) ions has revealed that both complexes have two additional water molecules bound to the central metal ions to complete the octahedral structure. The structure of the nickel(II) complex is similar both in crystals and in solution, whereas the bis(glycinato)zinc(II) in solution is coordinated with two water molecules instead of two neighboring glycinato carbonyl oxygen atoms in the solid state.

X-Ray and neutron diffraction techniques have long been used in the investigations of the structure of metal complexes in solution.[1,2] In recent years the EXAFS (extended X-ray absorption fine structure) spectroscopy has been proved to be successful for studies of the short-range order of atoms in solution.[3-5] From both diffraction and EXAFS methods can be obtained structural information related to the radial distribution of atom pairs in a system; the number of neighboring atoms around a central atom, the interatomic distance between them and its root-mean-square deviation. However, there are some differences in the nature of information to be obtained from both methods. EXAFS data bear on the near-neighbor environment of an X-ray absorbing atom only, while scatterings of all atom pairs with different distances are detected by conventional diffraction techniques. Since the contribution of the structures of the solvent and solvated anions to the total diffraction pattern is very large particularly in dilute solutions, structural information on metal complexes may sometimes be hidden by it. The difficulity may be overcome by increasing the concentration of metal ions and by selecting an appropriate counter anion, however. The diffraction method thus has a limited use in the case of dilute solutions. In the EXAFS spectra, on the contrary, the contribution from the solvent structure is absent and the interaction of the nearest neighbors with an absorbing atom is most emphasized, and hence the EXAFS method may be the most suitable for structural determination of metal complexes of low concentration in solution.

According to the single-electron and single-scattering theory of the EXAFS,[6-8] it is essential in structural analysis to evaluate the backscattering amplitude of the scatterer and the phase shifts due to the absorber and scatterers. The method of estimation of these parameter values, as well as data reduction procedures, differs in different groups and laboratories. It seems ambiguous to what extent different treatments and analyses of EXAFS spectra affect the final structure data to be obtained. The first aim of the present study is, therefore, to examine uncertainties in structural data obtained by the EXAFS method. To this aim, EXAFS oscillations are extracted by using two different programs. The phase-shifts and the backscattering amplitudes are estimated either from Teo-Lee's values[9] based on pseudo *ab initio* calculations or from the EXAFS spectra of standard references of known structure. Least-squares fitting calculations are then made both in the reciprocal and in the real spaces on the basis of the various standard references.

The structure of the mono- and tris(glycinato) complexes of nickel(II),[10] copper(II),[11] and zinc(II)[12] ions in aqueous solutions has been determined by means of X-ray diffraction. However, the structure of the relevant bis(glycinato) complexes in solution is not determinable by the conventional X-ray analysis due to their low solubility in water (less than 0.3 mol dm^{-3}). The second aim is, therefore, to determine the structure of the bis(glycinato) complexes of nickel(II) and zinc(II) in solution by the EXAFS method. The solubility of the bis(glycinato)copper(II) complex in water was too low ($\approx$0.025 mol dm^{-3}) to determine the structure of the complex even by the present transmission mode EXAFS experiment.

Experimental

EXAFS Measurements. EXAFS spectra were measured on a laboratory X-ray absorption spectrometer consisting of a Johansson cut bent crystal (Ge(220)), a rotating anode generator (Rigaku Ru-200) and a fast solid-state detector. Details of the spectrometer have been described elsewhere.[13]

Samples measured were aqueous solutions containing the $[M(gly)_3]^-$ (1 mol dm^{-3}) or $[M(gly)_2]$ (0.1—0.3 mol dm^{-3}) (M= Ni(II), Zn(II), and gly=glycinate ion) complex as a main species, which were prepared in the same way as previously described.[10,12] Crystalline samples of the bis(glycinato) complexes of both metals, the structure of which has been investigated by an X-ray diffraction method,[15,16] were also measured for comparison. Aqueous metal nitrate solutions (1 mol dm^{-3}) containing haxaaqua ions and crystalline

TABLE 1. SAMPLES FOR EXAFS MEASUREMENTS

Sample	Species	Mole ratio C_{gly}/C_M	C_M/mol dm^{-3}
Powder A	NiO	0	—
Solution B	$[Ni(OH_2)_6]^{2+}$	0	1.023
Solution C	$[Ni(gly)_3]^-$	3.94	1.000
Solution D	$[Ni(gly)_2]$	2.00	0.1225
Powder E	$[Ni(gly)_2(OH_2)_2]$	2.00	—
Powder F	ZnO	0	—
Solution G	$[Zn(OH_2)_6]^{2+}$	0	1.004
Solution H	$[Zn(gly)_3]^-$	5.09	1.245
Solution I	$[Zn(gly)_2]$	2.00	0.2919
Powder J	$[Zn(gly)_2]\cdot H_2O$	2.00	—

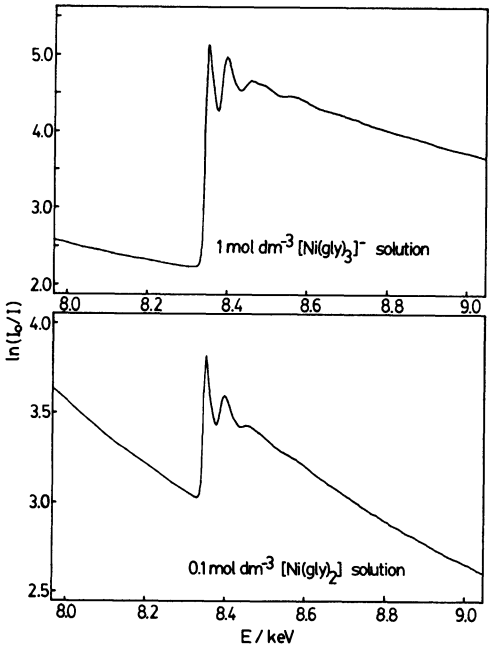

Fig. 1. The absorption spectra for the solutions containing the $[Ni(gly)_3]^-$ (upper part) and $[Ni(gly)_2]$ (lower part) complexes.

powders of the metal oxides were measured as structure standards.[14,17] Details of the samples are summarized in Table 1.

The solution samples were held between thin Mylar windows by the use of a spacer with an adequate thickness to obtain an effective jump at the absorption edge (μx=1—2 with the absorption coefficient μ and the sample thickness x). The powder samples were mixed and ground with boron nitride to dilute the sample, and finally pressed to thin pellets.

The absorbance μx is given as $\ln(I_0/I)$, where I and I_0 are the X-ray intensities with and without a sample, respectively. The intensities I_0 and I were measured at the same time by a partially transmitting ion chamber and an SSD, respectively. The data collection time for covering the required energy region was approximately 10 h and more than 1×10^7 counts of I_0 were obtained at each data point. Measurements were repeated at least twice in order to examine the reproducibility of the results.

An example of the absorption spectra for the solution samples containing high and low concentrations of main species ($[Ni(gly)_3]^-$ and $[Ni(gly)_2]$ complexes) is depicted in Fig. 1.

Data Reduction Procedure. The EXAFS data were analyzed by two different programs, *i.e.* ours (program I) and the one used in the Xerox Palo Alto Laboratory (program II).

Program I. Background absorption other than that for the K edge of an absorption atom of interest was evaluated by least-squares fitting Victoreen's formula[19] to the preedge and was subtracted from the total absorption by extrapolation. The smooth K-shell absorption μ_0 due to an isolated atom was estimated by fitting a smooth curve to the observed absorption spectrum using a cubic spline function.[20] Two or three knots over the whole region were enough to give a good approximation for μ_0.

The modulation $\chi(k)$ was extracted and normalized by the following equation;

$$\chi(k) = \{\mu(k)-\mu_0(k)\}/\mu_0(k) \quad (1)$$

where k is the photoelectron wave vector ejected and is given as $\sqrt{2m(E-E_0)/\hbar^2}$. E denotes the energy of the incident X-rays and E_0 is the binding energy of a K-shell electron.

Program II. Details of the data treatments are referred to the literature.[18] Background absorption was approximated with a function of $A+B\cdot E^{-p}$, where A, B, and p were empirical parameters which were determined by a least-squares fit to the absorption data below the K-edge of interest. In practice, p is found to be between 1 and 3, consistent with Victoreen's formula used in program I. The EXAFS pattern was extracted by assuming a 6th-order polynomial function for the smooth K-shell absorption μ_0.

The $k\cdot\chi(k)$ values obtained by both programs are compared in Fig. 2. As seen in Fig. 2, an approximation of μ_0 by either program I or II is equally good for the extraction of $\chi(k)$. The oscillation of the EXAFS data weighted by k^n was converted by the Fourier transformation into the radial distribution in the r-space as

$$\phi(r) = \sqrt{(1/2\pi)}\int_{k_{min}}^{k_{max}} k^n\cdot\chi(k)\cdot W(k)\cdot\exp(-2ikr)\mathrm{d}k. \quad (2)$$

Here $W(k)$ is the window function to reduce ripples due to the truncation effect. The window functions employed in programs I and II were, respectively, of the Hanning type[21] and of Gaussian type. The resulting $\phi(r)$ values obtained with n=2 by using program I are shown in Fig. 3.

Least-squares Calculation. The structure parameters (interatomic distances, mean square displacements and coordination numbers) were obtained by comparing the observed EXAFS spectra and the model function given by the single scattering theory[6-8,22] as,

$$\chi(k)_{calcd} = \sum_j\{n_j/(k\cdot r_j^2)\}\exp(-2\sigma_j^2k^2)B_jF_j(\pi, k) \times\sin(2kr_j+\alpha_j(k)), \quad (3)$$

where $F_j(\pi,k)$ is the backscattering amplitude from each of n_j scatterers j at distance r_j from the X-ray absorbing atom. σ_j^2 is the mean square displacement of the equilibrium distance r_j and B_j is the amplitude reduction factor related to inelastic losses at the absorbing atom due to the many-body effect.[22] $\alpha_j(k)$ is the total scattering phase shift experienced by the photoelectron.

The observed spectra can be compared with the theoretical ones by a least-squares procedure in either r- or k-space. The

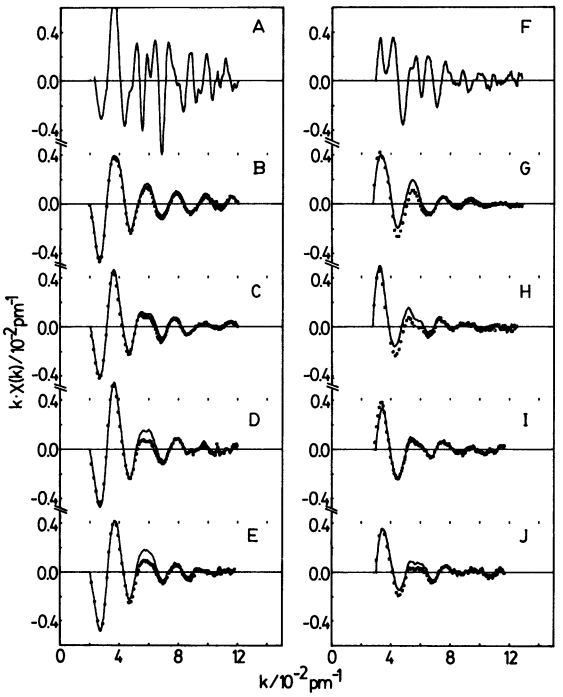

Fig. 2. The EXAFS spectra for the samples measured. The solid lines and the dots were obtained, respectively, by the cubic spline fits (program I) and the 6th-order polynomial fits (program II). A: NiO powder, B: $[Ni(OH_2)_6]^{2+}$ in solution, C: $[Ni(gly)_3]^-$ in solution, D: $[Ni(gly)_2]$ in solution, E: $[Ni(gly)_2(OH_2)_2]$ powder, F: ZnO powder, G: $[Zn(OH_2)_6]^{2+}$ in solution, H: $[Zn(gly)_3]^-$ in solution, I: $[Zn(gly)_2]$ in solution and J: $[Zn(gly)_2]\cdot H_2O$ powder.

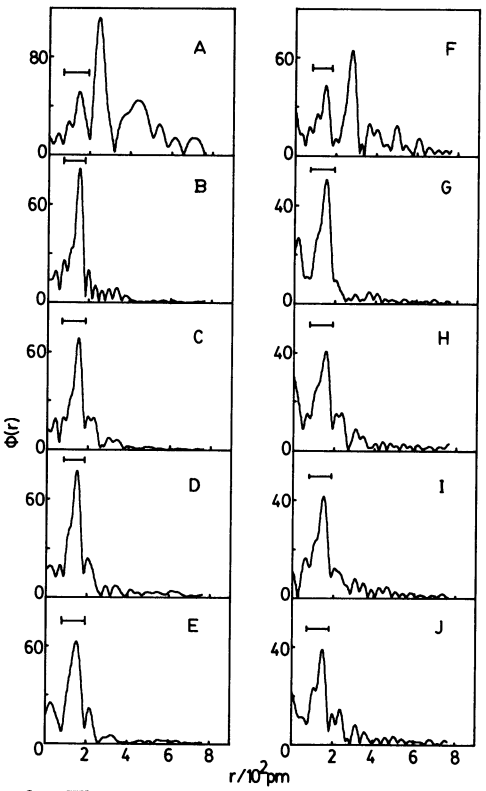

Fig. 3. The Fourier transform $\phi(r)$ of the EXAFS spectra shown in Fig. 1, uncorrected for the phase shifts. The bars indicate the r-range of the inverse Fourier transform shown in Fig. 4 (dots).

latter procedure needs an additional Fourier backfiltering of the peak of interest in the $\phi(r)$ curve. Theoretically both analyses in the k- or r-space should give equivalent results.

We examined least-squares calculations both in the r- and k-spaces.

Analysis in the k-*Space (program I).* A curve fitting procedure in the k-space was applied to the Fourier filtered $k^2\cdot\chi(k)_{obsd}$ values to minimize the error-square sum U_1,

$$U_1 = \sum_{k_{min}}^{k_{max}} k^4(\chi(k)_{obsd} - \chi(k)_{calcd})^2. \quad (4)$$

The values of $F_j(\pi,k)$ and $\alpha_j(k)$ for $\chi(k)$ in Eq. 3 were quoted from the tables reported by Teo and Lee.[9] The values are given against the absolute k-values and thus an improper evaluation of E_0 should result in a systematic distortion of the k-scale and affect the interatomic distances to be determined. Furthermore, the theoretical values of the backscattering amplitudes $F_j(\pi,k)$ are usually larger by *ca.* 50% than those observed,[23] which sometimes give unreasonable bond lengths between an X-ray absorbing central atom and its neighboring ones and the coordination numbers. In this procedure the parameters E_0 and B were estimated from the standard samples of known structure (here we employed the $[M(OH_2)_6]^{2+}$ and MO (M^{2+}=Ni^{2+} and Zn^{2+})) and then they were used as constant values in the course of the analysis of the EXAFS spectra of unknown samples, while r, σ, and n were refined as variables.

Analysis in the r-*Space (program II).* The analysis of the first peak in the r-space followed the procedure, the details of which have been described elsewhere.[18] The E_0 values were fixed to the values estimated in the previous section. The essential formulae are described below.

The $\phi(r)$ values can be expressed by the convolution of two functions as

$$\phi_j(r) = \sum_j \int_0^\infty \frac{dr'}{r'^2} p_{ij}(r')\xi_{ij}(r-r'). \quad (5)$$

$p_{ij}(r)$ is the pair correlation function and ξ_{ij} is the peak function which contains the information on the electron scattering process such as the backscattering amplitude, photoelectron phase-shift and so on. The pair correlation function was assumed to be a Gaussian expressed by

$$p_{ij}(r) = n_j\sqrt{(2\pi\sigma_j^2)}\exp[-(r-r_j)^2/2\sigma_j^2]. \quad (6)$$

The peak function ξ_{ij} including the phase-shifts and the backscattering amplitudes can be empirically extracted from the $\phi(r)$ values of the standard references of known structure according to Eqs. 5 and 6. Since the ξ_{ij} is insensitive to crystal structure, local bonding, *etc.*,[18] the ξ_{ij} values thus evaluated were adopted in the structure analysis of unknown samples. The model function $\phi_m(r)$ for unknown samples was calculated by using Eq. 5 with the ξ_{ij} values.

The curve fits were carried out by comparing the real (Re) and the imaginary (Im) parts of the $\phi(r)$ with $\phi_m(r)$ values to minimize the error-square sum U_2,

$$U_2 = (2N)^{-1}\sum^N \{\mathrm{Re}(\phi-\phi_m)^2/[(\mathrm{Re}\phi)^2+\{\mathrm{Re}(d\phi/dr)\}^2] + \mathrm{Im}(\phi-\phi_m)^2/[(\mathrm{Im}\phi)^2+\{\mathrm{Im}(d\phi/dr)\}^2]\}. \quad (7)$$

In the course of the calculation, parameters of the radial shift Δr, additional broadening $\Delta\sigma$ and coordination number n were allowed to vary as independent variables. The bond length of the structural references was fixed at the values established from the X-ray diffraction method.

Raman Spectroscopic Measurement. Raman spectra for the bis(glycinato)zinc(II) complex in the solid and solution states were measured with a JEOL laser Raman spectrometer JRS-S1 with the use of the 514.5 nm excited line of Ar^+ laser.

Results and Discussion

Selection of Structure Standards. In order to examine the applicability of the structural standard to the structure analysis of complexes in solution, we examined the spectra of crystalline powder of metal oxides and aqueous metal nitrate solutions containing hexaaqua $[M(OH_2)_6]^{2+}$ ions, the structure of both species having been known.[14,17] The EXAFS spectra $k\cdot\chi(k)$ and the Fourier-transformed function $\phi(r)$ for the structure references are shown in Figs. 2 (A, B, F, and G) and 3 (A, B, F, and G), respectively. In the course of the least-squares fits in the k-space (program I) for the M–O signature within the crystalline metal oxides and within the $[M(OH_2)_6]^{2+}$ in the solutios, parameters E_0, B, and σ were all allowed to vary simultaneously, while the coordination number n was fixed at the known value (6 for NiO, 4 for ZnO and 6 for the aquanickel(II) and -zinc(II) ions). The values for the central atom phase-shift of atom M and those for the backscattering phase-shift and amplitude of atom O were taken from the theoretical values by Teo and Lee. The M–O distance r, which has been determined by the X-ray diffraction method,[14,17] was also allowed to vary in order to check the reproducibility of the value. The results are given in Table 2. The values of E_0 thus estimated agreed with each other in the standard substances of a given metal and seemed reasonable because the interatomic distances converged to the literature values.[14,17] However, the B values obtained for the metal oxides were smaller by a factor of 1.2—1.5 than those for the aqueous solutions. This leads to 20—50% larger coordination number when we use the metal oxides as a standard for the analysis of unknown samples than one uses the solution standard, although the bond length determined may be independent of the selection of the references. Agreements between experimental and calculated $k^2\cdot\chi(k)$ curves are shown in Fig. 4 (A, B, F, and G).

Least-squares fits in the r-space, in which the $\phi(r)$ peak due to the M–O bonds within the $[M(OH_2)_6]^{2+}$ ions were compared with those of the M–O bonds in the metal oxides as the standard, gave larger coordination number than the correct value of six, whereas the bond lengths obtained were in good agreement with those determined by the X-ray diffraction method.

Thus, we concluded that the metal nitrate solutions were more suitable structural references for the solution samples than the metal oxides, even though both of them have the same coordination atoms at the similar distance.

TABLE 2. COMPARISON OF E_0 AND B VALUES OBTAINED BY THE LEAST-SQUARES FITS FROM DIFFERENT STANDARD MATERIALS. STANDARD DEVIATIONS ARE GIVEN IN PARENTHESES

Material	E_0/eV	10^3B	r/pm	σ/pm	$r_{X\text{-}ray}$/pm
$Ni(NO_3)_2$ solution	8349(1)	393(3)	202(1)	1.4(5)	204[a]
NiO powder	8348(1)	258(6)	208(1)	3.1(6)	208[b]
$Zn(NO_3)_2$ solution	9674(1)	406(3)	207(1)	6.5(3)	208[a]
ZnO powder	9675(1)	353(5)	196(1)	3.8(4)	194—197[b]

a) Ref. 14. b) Ref. 17.

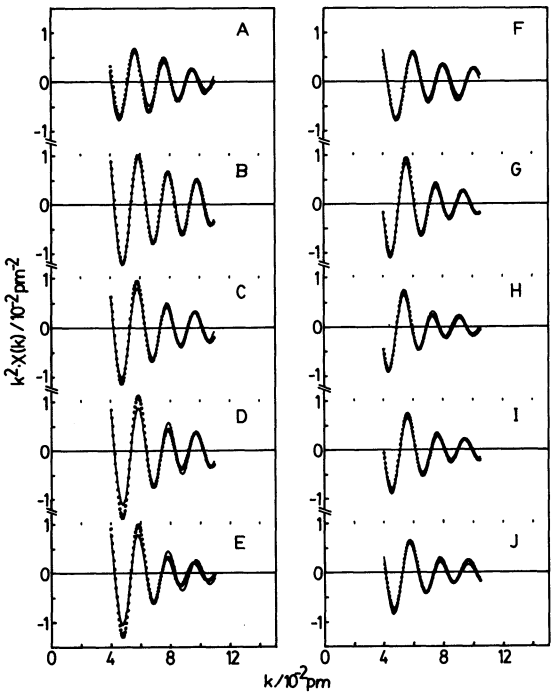

Fig. 4. The Fourier filtered $k^2\cdot\chi(k)$ curves of the main peak depicted in Fig. 3. The dotted and solid lines represent, respectively, the observed and calculated values by using parameter values in Tables 3 and 4.

In the course of the analysis of the EXAFS spectra of glycinato complexes by adopting the phase-shifts empirically evaluated, they should be evaluated from compounds of well established structure including M–O and M–N bonds. However, since phase shifts can be well approximated to be the same for atoms having similar number of electrons,[24] the phase-shift of the backscattering atom N (sometimes even atom C) was assumed to be the same as that of atom O, which was evaluated from the $[M(OH_2)_6]^{2+}$ ions.

Ni(II) Complexes. The $k\cdot\chi(k)$ curves and the $\phi(r)$ values of the solution samples containing the tris- and bis(glycinato) complexes and the crystalline powders of the bis(glycinato) complex are depicted in Figs. 2 (C, D, and E) and 3 (C, D, and E), respectively.

Table 3. Results of the curve fits for the nickel (II)–glycinato complexes with distance r and root-mean-square displacement σ. $\Delta\sigma$ denotes the difference between the sample and the standard $[Ni(OH_2)_6]^{2+}$. Standard deviations are given in parentheses

Complex	Scatterer	Program I		Program II		X-ray
		r/pm	σ/pm	r/pm	$\Delta\sigma$/pm	
$[Ni(OH_2)_6]^{2+}$(aq)	O	202(1)	1.4(5)	204[b]	—	204[c]
$[Ni(gly)_3]^-$(aq)	O or N	205(1)	5.5(1)	209	6.4	
	O	201(1)	1.4[a]	204	0.0	203[d]
	N	210(1)	1.4[a]	212	8.0	214[d]
$[Ni(gly)_2(OH_2)_2]$(aq)	O or N	204(1)	3.7(3)	204	3.4	
$[Ni(gly)_2(OH_2)_2]$(c)	O or N	204(1)	4.7(4)	205	4.7	210[e] (2×Ni–OH_2)
						206[e] (2×Ni–O)
						208[e] (2×Ni–N)

a) The values were kept constant during the calculation. b) Employed as a standard from Ref. 14. c) Ref. 14. d) Ref. 10. e) Ref. 15.

A small but significant shoulder at about 6×10^{-2} pm^{-1} appearing in the $k\cdot\chi(k)$ curves of samples C, D, and E, which has not been observed in solution B, indicated that there should be at least two interactions with different distances contributing to the EXAFS oscillations.

In the $\phi(r)$ curve for sample solution C containing the tris(glycinato)nickelate(II) complex as the predominant species, two peaks were observed at about 150 and 220 pm. The first peak at 150 pm was ascribable to the first neighbor Ni–O and Ni–N pairs within the $[Ni(gly)_3]^-$ complex. The small and slightly split second peak at 220 pm was not significantly affected by different estimations of the smooth background μ_0 and the selections of k_{min} and k_{max} values for the Fourier transformation, and hence it indicated a significant signature. The peak might be assignable to the next nearest neighbor Ni···C distance within the tris(glycinato) complexes, although the peak might also contain a spurious one due to the truncation effect of the Fourier transform.

Firstly, the predominant peak at 150 pm, indicated by a bar in the figure, was analyzed by using the least-squares method in the k-space for the Fourier filtered $k^2\cdot\chi(k)$ values. Theoretical values by Teo and Lee[9] were used for the phase-shifts and the backscattering functions in combination with program I. The coordination number was fixed to the known value (n=6). The model of only one backscatterer (O or N) gave a satisfactory agreement between the calculated and observed $k^2\cdot\chi(k)$ values with the bond length of 205 pm and the σ value of 5.5 pm. However, the σ value estimated from this model was about four times larger than that (1.4 pm) obtained for the Ni–O bond within the reference $[Ni(OH_2)_6]^{2+}$ ion (see Table 3). The σ value thus obtained for the Ni–O and Ni–N bonds within the $[Ni(gly)_3]^-$ complex seemed unreasonably large, because the temperature factors for the Ni–O and Ni–N bonds within the complex were virtually the same as that of the Ni–OH_2 bond within the $[Ni(OH_2)_6]^{2+}$ complex.[10,14] Therefore, we assumed that the σ values of the both Ni–O and Ni–N were the same as the value of the standard hexaaqua complex (σ=1.4 pm) and allowed the lengths of the both Ni–O and Ni–N bonds to vary independently. As a result, the least-squares calculation converged to two different lengths of the Ni–O (201 pm) and Ni–N (210 pm) bonds, independent of the initial value inserted for the lengths of the two bonds (Table 3).

A similar consideration was examined in the data analysis in the r-space. The first peak at 150 pm was directly analyzed in the r-space by using program II by assuming one and two Gaussian models, the peak due to the Ni–O bonds within the $[Ni(OH_2)_6]^{2+}$ being employed as the standard. The results are given in Table 3.

As seen in Table 3, both calculations for the data in the k- and r-spaces gave similar results that under the assumption of one kind of the bond length the Ni–O and Ni–N distances were 205—209 pm, while the Ni–O and Ni–N bond lengths were 201—204 and 210—212 pm, respectively, under the assumption of two different lengths for the Ni–O and Ni–N bonds. The difference in calculations between two programs I and II was less than 3 pm, which was compared with the difference in the standard Ni–O distance estimated by the different programs for the $[Ni(OH_2)_6]^{2+}$ ion.

The analysis of the first peak both in the k- and r-spaces thus gives almost the same results and thus errors caused by a Fourier backfiltering are within experimental errors. In addition, the choice of either theoretical or empirical values for the phase-shifts and backscattering amplitudes does not significantly affect the result as long as suitable standard samples are adopted in order to obtain reasonable E_0 and B values. We can recommend to employ the $[Ni(OH_2)_6]^{2+}$ complex in solution as the standard rather than NiO in the course of the structural analysis of the $[Ni(gly)_3]^-$ in solution, because the former standard gives a better B value leading to more reasonable coordination number of the complexes in solution.

The present EXAFS analysis by using both programs I and II gave the results consistent with those from X-ray diffraction.[10]

The analysis of the second peak at 220 pm was not possible because it was too small to apply the curve-fit

TABLE 4. RESULTS OF THE CURVE FITS FOR THE ZINC(II)-GLYCINATO COMPLEXES WITH DISTANCE r AND ROOT-MEAN-SQUARE DISPLACEMENT σ. $\Delta\sigma$ DENOTES THE DIFFERENCE BETWEEN THE SAMPLE AND THE STANDARD $[Zn(OH_2)_6]^{2+}$. STANDARD DEVIATIONS ARE GIVEN IN PARENTHESES

Complex	Scatterer	Program I		Program II		X-ray
		r/pm	σ/pm	r/pm	$\Delta\sigma$/pm	
$[Zn(OH_2)_6]^{2+}$(aq)	O	207(1)	6.5(3)	208[b]	—	208[c]
$[Zn(gly)_3]^-$(aq)	O or N	213(1)	6.8(1)	214	7.7	
	O	213(1)	6.5[a]	210	0.2	212[d]
	N	213(1)	6.5[a]	219	8.9	212[d]
$[Zn(gly)_2(OH_2)_2]$(aq)	O or N	207(1)	6.6(2)	208	5.5	
$[Zn(gly)_2]\cdot H_2O$(c)	O or N	203(1)	7.0(3)	204	8.7	

a) The values were kept constant during the calculation. b) Employed as a standard from Ref. 14. c) Ref. 14. d) Ref. 12.

procedure, although we could approximately estimate the Ni···C distance to be about 280 pm from the peak position after the correction for the phase-shift, which reasonably agreed with the literature value determined by means of solution X-ray diffraction (290 pm).[10]

The same analytical procedure was applied to the solution and powder samples of the bis(glycinato)nickel(II) complex. The amplitude of the first peak in the Fourier transform was similar in both samples (Fig. 3, D and E) and hence the curve-fits gave very similar results (Table 3), which implied that the environment of the Ni(II) ions should be very similar in both states. Therefore, the bis(glycinato)nickel(II) in the aqueous solution was expected to have a six-coordination with two additional water molecules to complete the octahedral configuration as in the crystalline state.[12] A mean value (208 pm) of the distances found in the X-ray crystallographic investigation[15] was slightly longer than the value found by the EXAFS measurement (204 pm for the average bond length), but the difference was almost within uncertainties of the latter.

Zinc(II) Complexes. The $k\cdot\chi(k)$ and $\phi(r)$ values of the solution samples containing the tris- and bis(glycinato) complexes and of the bis(glycinato)-zinc(II) complex in powder are shown in Figs. 2 and 3 (H, I, and J). The predominant first peak at 150 pm in Fig. 3 (H, I, and J) are due to the first neighbor Zn–O and Zn–N bonds within the glycinato complexes.

The structure of the Zn(II)-glycinato complexes was analyzed in the same manner as decribed in the previous section for the nickel(II) complexes. For solution H containing the $[Zn(gly)_3]^-$ complex as a predominant species, the least-squares calculations for the first peak at 150 pm in the $\phi(r)$ curve (Fig. 3H) were performed both in the k- and r-spaces with two models with the same length for the Zn–O and Zn–N bonds and with the different lengths of the two bonds. Both model calculations gave the similar results (see Table 4). The interatomic distances thus determined are consistent with those reported in an X-ray diffraction study.[12]

The structure of the bis(glycinato)zinc(II) complex in the solid state was reported to be apically distorted octahedral with additional two carbonyl oxygen atoms within the glycinate ions coordinated to adjacent Zn(II) ions,[16] although the complete structural analysis was not yet achieved. Bis-complexes of zinc(II) ion with various bidentate ligands are known to have the tetrahedral structure. However, as is seen in Fig. 3 (I and J) the amplitude of the first peak for both solution and powder samples is very similar, which indicates a similar coordination number for the bis-complex in both states. The curve fit analysis in the k-space for the first peak in Fig. 3I gave the coordination number of nearly six independent of the initial value at the least-squares approach. Thus, it was concluded that the bis(glycinato)zinc(II) complex has an octahedral structure with two additional water molecules in aqueous solution.

The mean bond distance (203 pm) for the powder sample seemed to be slightly shorter than that found in the solution (207 pm). This trend was not observed in the case of the bis(glycinato)nickel(II) complexes.

In Raman spectral measurements of the Zn–N stretching frequency in the bis(glycinato)zinc(II) complex the band observed at $(467\pm5)\,cm^{-1}$ in the crystal shifted to $(434\pm5)\,cm^{-1}$ in the aqueous solution. The shift of the Zn–N stretching frequency by *ca.* $33\,cm^{-1}$ found in the present study has also been reported by Krishnan and Plane,[23] which suggested lengthening of the Zn–N bond in the solution state. The longer Zn–N bond in solution than in crystal found in the present EXAFS study may correspond to the shift of the Zn–N stretching frequency toward the lower frequency side in the Raman spectra in solution. The weakening of the Zn–N bond (and probably in the Zn–O bond, too) of the bis(glycinato)zinc(II) complex in solution compared with that in crystal may be caused by a stronger electron donation from coordinated water molecules in the bis-complex in solution than that from carbonyl oxygen atoms in the solid state.

This work was supported by the Joint Studies Program (1983—1984) of the Institute for Molecular Science and by the Grant-in-Aid for Scientific Reseach No. 57470054 from the Ministry of Education, Science and Culture. The authors (T. Y. and H. O.) thank Dr. J. B. Boyce (Xerox Palo Alto Reseach Centers) for his kind help in using their computer program and his valuable

discussion. A part of the calculations was carried out at the Institute for Molecular Science in Okazaki.

References

1) H. Ohtaki, *Rev. Inorg. Chem.*, **4**, 103 (1982).
2) J. E. Enderby and G. W. Neilson., *Rep. Prog. Phys.*, **44**, 38 (1981).
3) D. R. Sandstrom, B. R. Stults, and R. B. Greegor, "Structural Evidence for Solutions from EXAFS Measurements," in "EXAFS Spectroscopy," ed by B.-K. Teo and D. C. Joy, Plenum Press, New York (1981), Chap. 9, pp. 139—157.
4) T. Yamaguchi, O. Lindqvist, J. B. Boyce, and T. Claeson, "EXAFS, X-Ray and Neutron Diffraction of Electrolyte Solutions," in "EXAFS and Near Edge Structure III," ed by K. O. Hodgson, B. Hedman, and J. E. Penner-Hahn, Springer-Verlag, Berlin (1984), pp. 417—419.
5) M. Sano, T. Maruo, and H. Yamatera, *Bull. Chem. Soc. Jpn.*, **57**, 2757 (1984).
6) D. E. Sayers, E. A. Stern, and F. W. Lytle, *Phys. Rev. Lett.*, **27**, 1204 (1971).
7) E. A. Stern, *Phys. Rev. B*, **10**, 3027 (1974).
8) E. A. Stern, D. E. Sayers, and F. W. Lytle, *Phys. Rev. B*, **11**, 4836 (1975).
9) B.-K. Teo and P. A. Lee, *J. Am. Chem. Soc.*, **101**, 2815 (1979).
10) K. Ozutsumi and H. Ohtaki, *Bull. Chem. Soc. Jpn.*, **56**, 3635 (1983).
11) K. Ozutsumi and H. Ohtaki, *Bull. Chem. Soc. Jpn.*, **57**, 2605 (1984).
12) K. Ozutsumi and H. Ohtaki, *Bull. Chem. Soc. Jpn.*, **58**, 1651 (1985).
13) K. Tohji, Y. Udagawa, T. Kawasaki, and K. Masuda, *Rev. Sci. Instrum.*, **54**, 1482 (1983).
14) H. Ohtaki, T. Yamaguchi, and M. Maeda, *Bull. Chem. Soc. Jpn.*, **49**, 701 (1976).
15) H. C. Freeman and J. M. Guss, *Acta Crystallogr., Sect. B*, **24**, 1133 (1968).
16) B. W. Low, F. L. Hirshfeld, and F. M. Richards, *J. Am. Chem. Soc.*, **81**, 4412 (1959).
17) R. W. G. Wyckoff, "Crystal Structures," Interscience, New York (1964), Vol. 1.
18) J. B. Boyce, T. M. Hayes, and J. C. Mikkelsen, Jr., *Phys. Rev., B*, **23**, 2876 (1981).
19) "International Tables for X-Ray Crystallography," Kynoch Press, Vol. III, p. 161.
20) P. A. Lee, P. H. Citrin, P. Eisenberger, and B. M. Kincaid, *Rev. Mod. Phys.*, **53**, 769 (1981).
21) F. J. Harris, *Proc. IEEE*, **66**, 51 (1978).
22) B. Lengeler and P. Eisenberger, *Phys. Rev., B*, **21**, 4507 (1980).
23) J. J. Rehr, E. A. Stern, R. L. Martin, and E. R. Davidson, *Phys. Rev., B*, **17**, 560 (1978).
24) T. Yamaguchi, O. Lindqvist, J. B. Boyce, and T. Claeson, *Acta Chem., Scand., Ser., A*, **38**, 423 (1984).
25) K. Krishnan and R. A. Plane, *Inorg. Chem.*, **6**, 55 (1967).